JOURNAL OF THEORETICAL AND APPLIED MECHANICS
60, 1, pp. 3-16, Warsaw 2022
https://doi.org/10.15632/jtam-pl/143297

A SIMPLIFIED ELLIPTICAL FUNCTION SOLUTION FOR COUPLED NONLINEAR VIBRATION OF MULTILAYER GRAPHENE SHEETS

G. Venkatraman, D. Suji

PSG College of Technology, Department of Civil Engineering, Coimbatore, India

e-mail: gvr.civil@psgtech.ac.in; dsu.civil@psgtech.ac.in

This paper presents a simple exact solution for coupled nonlinear free vibration analysis of Multilayer Graphene Sheets (MLGS) using elliptical functions. Though elliptical functions are used in nonlinear dynamics, they are employed to find the exact solution of a coupled system for the first time. The nonlinear dynamic equation including geometric nonlinearity and Eringen nonlocal theory is uncoupled by elliptical functions, and exact solutions for simply supported boundary conditions are obtained. The results are compared with the harmonic balance method. The nonlinear frequency of MLGS is studied for its effects with a small scale parameter, and the linear and nonlinear van der Waals force.

Keywords: nonlinear coupled vibration, nonlinear van der Waals force, Multilayer Graphene Sheets, elliptical function, exact solution

1. Introduction

Graphene is defined as a flat one-atom-thick of carbon tightly packed into a two-dimensional lattice. Graphene sheets have attracted much attention of researchers because of its promising mechanical and electrical properties. These properties of graphene sheets lead to the usage of innovative applications in many fields.

The high stiffness to inertia ratio of graphene sheets attracted research in high frequency nanomechanical devices. Experimental investigation and characterization of graphene sheets at nanoscale are hard to achieve. To overcome this difficulty, many analytical and numerical methods have been developed. Initially, numerical methods such as molecular dynamics (MD) simulations etc., are used to investigate. Though these methods have good agreement with test results, they require large amount of computational resources. Continuum based methods are developed to analyse the nanoscale graphene sheets.

Initially, He *et al.* (2005) and Behfar and Naghdabadi (2005) studied dynamic behaviour of Multilayer Graphene Sheets by classical elasticity theory. Since nonlocal effects had significant influence on dynamic behaviour, nonlocal models were used to study the behaviour of SLGS by Murmu and Pradhan (2009). Pradhan and Phadikar (2009) investigated vibration characteristics of Single Layer Graphene Sheet (SLGS) and Bilayer Graphene Sheets (BLGSs) using nonlocal classical plate theory (CLPT) and the first order shear deformation theory (FSDT). Based on nonlocal continuum theory and Molecular Dynamic (MD) simulations, Arash and Wang (2011) reported free vibration characteristics of SLGS and BLGS.

Other than nonlocal elastic theories, strain gradient theory and couple stress theory used to study the vibration of nanostructures. Strain gradient elasticity theory proposed by Lam *et al.* (2003) was used to find the behaviour of nanomaterials. Kong *et al.* (2009) used strain gradient elasticity theory to static and dynamic analysis of microbeams. Timoshenko beam model based on strain gradient elasticity theory was solved by Wang *et al.* (2010). Ghayesh and Farokhi (2015) analysed nonlinear dynamics of microplates using modified couple stress theory

and found different response amplitudes. Asghari (2012) used modified couple stress theory to model geometrically nonlinear microplates.

Ghannadpour and Moradi (2019) used the semi Galerkin method to analyse nanographene sheets under compression. Using higher-order nonlocal strain gradient theory, Nematollahi and Mohammadi (2019) analysed geometrically nonlinear vibration of sandwich nanoplates. Many approximate methods have been used to find solutions of nonlinear nonlocal dynamics of graphene sheets. The finite element method was used to solve nonlinear GS vibration by Ansari *et al.* (2010). Mianroodi *et al.* (2011) used the finite difference method to solve dynamic behaviour of graphene sheets.

The computational cost of the nonlocal elasticity is less than that of strain gradient theories due to the fact that strain gradient terms are also incorporated (Farajpour *et al.*, 2018). The strain gradient theories are required when the stiffness hardening is considered and length of the graphene sheet is large (Farajpour *et al.*, 2018). Otherwise, nonlocal elasticity itself is sufficient at a lesser computational cost. In our study, we apply nonlocal elasticity theory because the strain hardening effects are not considered.

The methods available to solve the coupled nonlinear vibration analysis of MLGS (like Harmonic Balance Method, Method of Multiple Scales, Finite Element Method, etc.) are based on trigonometric trial functions. Since cubic nonlinearity in stiffness is involved due to large amplitude vibration, a trigonometric trial function for time dependent displacements can give approximate results for small nonlinearities. An increase in nonlinearity will increase the error involved for the trigonometric trial functions. The exact solutions derived in this article can solve the strongly nonlinear coupled dynamic analysis more effectively than other trigonometric function based methods. To the best of the authors knowledge, the analytical solutions of nonlinear coupled free vibration analysis of MLGS with a higher order van der Waals force are presented for the first time.

2. Formulation

Figure 1 shows the MLGS modelled as nanoplates, with length a, breadth b and thickness of each layer h with the origin of the coordinate system at the center of the sheet. The Triple Layer Graphene Sheet (TLGS), each sheet modelled as a plate with the van der Waals force acting between them is shown in Fig. 2.

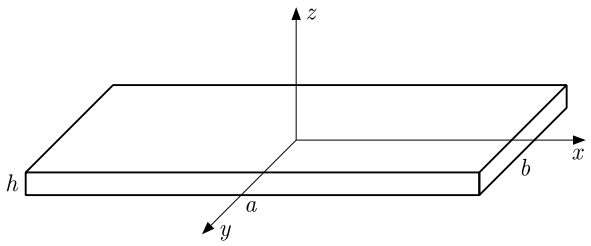

Fig. 1. Coordinate system for a graphene sheet modelled as plate

The small scale effects are significant in vibration of graphene sheets, Eringen nonlocal continuum theory is used. Based on the nonlocal continuum theory of Eringen, "stress at a point depends on the strain field at every point in the body". The relationship between the nonlocal stress tensor $\boldsymbol{\sigma}'$ and the local stress tensor $\boldsymbol{\sigma}$ is expressed as

$$[1-(e_0a)^2\nabla^2]\boldsymbol{\sigma}=\boldsymbol{\sigma}' \tag{2.1}$$

where (e_0a) is the small scale parameter, e_0 is a constant, and ∇^2 is the Laplacian operator.

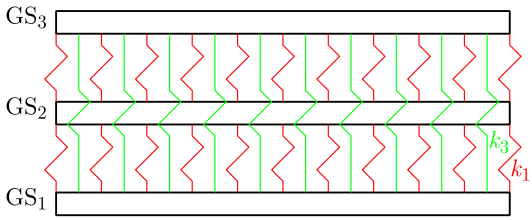

Fig. 2. Triple layer graphene sheet

The interaction between graphene sheets in MLGS is governed by the van der Waals force, which is derived from the Leonard-Jones potential

$$U_v = 4\epsilon_v\Big[\Big(\frac{\sigma_v}{d_v}\Big)^{12} - \Big(\frac{\sigma_v}{d_v}\Big)^{6}\Big] \tag{2.2}$$

where ϵ_v is bond energy at the equilibrium distance (which is equal to 0.002390 eV for carbon atoms of the graphene sheets), σ_v is a parameter determined by the equilibrium distance, and d_v is the distance between carbon atoms. Taking derivative of the Leonard-Jones Potential and expanding through Taylor series up to third order, the van der Waals force per unit area is obtained as (Jomehzadeh *et al.*, 2012)

$$F_i = \sum_{j=1,\, j\neq i}^{N} [c_{ij}(w_i - w_j) + \overline{c}_{ij}(w_i - w_j)^3] \tag{2.3}$$

The van der Waals coefficients are

$$\begin{aligned} c_{ij} &= -\Big(\frac{4\sqrt{3}}{9a_v^2}\Big)^2 \frac{24\epsilon_v}{\sigma_v^2}\Big(\frac{13\pi\sigma_v^{14}}{3h_v^{12}} - \frac{7\pi\sigma_v^8}{3h_v^6}\Big) \\ \overline{c}_{ij} &= -\Big(\frac{4\sqrt{3}}{9a_v^2}\Big)^2 \frac{336\epsilon_v}{\sigma_v^4}\Big(\frac{65\pi\sigma_v^{16}}{6h_v^{14}} - \frac{2\pi\sigma_v^{10}}{h_v^8}\Big) \end{aligned} \tag{2.4}$$

here, h_v is the distance between the graphene layers and N is the number of graphene layers.

Consider a simply supported MLGS of N layers. According to classical plate theory (CLPT), for i-th layer of MLGS, the displacements of an arbitrary point in the x, y, and z directions are given as

$$\begin{aligned} \overline{u}_i(x,y,z,t) &= u_i(x,y,t) - z\frac{\partial w_i(x,y,t)}{\partial x} \\ \overline{v}_i(x,y,z,t) &= v_i(x,y,t) - z\frac{\partial w_i(x,y,t)}{\partial y} \\ \overline{w}_i(x,y,z,t) &= w_i(x,y,t) \end{aligned} \tag{2.5}$$

where $u_i(x,y,t)$, $v_i(x,y,t)$ and $w_i(x,y,t)$ are the mid plane displacements of an arbitrary point in the i-th layer in the direction x, y, and z directions, respectively. The subscript i for a variable denotes the variable for the i-th layer of MLGS.

Von Karman strain displacement relationships are used to account the large deformation effect of graphene sheets. The strain components of the above displacement fields, including Von Karman nonlinear strain-displacement relationships are expressed as

$$\begin{aligned} &\varepsilon_{ix} = \varepsilon_{ix0} + z\kappa_{ix} \qquad \varepsilon_{iy} = \varepsilon_{iy0} + z\kappa_{iy} \\ &\gamma_{ixy} = \gamma_{ixy0} + z\kappa_{ixy} \end{aligned} \tag{2.6}$$

where ε_{ix0}, ε_{iy0}, γ_{ixy0} are the mid-plane strains, and κ_{ix}, κ_{iy}, κ_{ixy} are the curvatures defined as

$$\begin{Bmatrix} \varepsilon_{ix0} \\ \varepsilon_{iy0} \\ \gamma_{ixy0} \end{Bmatrix} = \begin{Bmatrix} \dfrac{\partial u_i}{\partial x} + \dfrac{1}{2}\Big(\dfrac{\partial w_i}{\partial x}\Big)^2 \\ \dfrac{\partial v_i}{\partial y} + \dfrac{1}{2}\Big(\dfrac{\partial w_i}{\partial y}\Big)^2 \\ \dfrac{\partial u_i}{\partial y} + \dfrac{\partial v_i}{\partial x} + \dfrac{\partial w_i}{\partial x}\dfrac{\partial w_i}{\partial y} \end{Bmatrix} \qquad \begin{Bmatrix} \kappa_{ix} \\ \kappa_{iy} \\ \kappa_{ixy} \end{Bmatrix} = \begin{Bmatrix} -\dfrac{\partial^2 w_i}{\partial x^2} \\ -\dfrac{\partial^2 w_i}{\partial y^2} \\ -2\dfrac{\partial^2 w_i}{\partial x \partial y} \end{Bmatrix} \tag{2.7}$$

The strain energy U of the MLGS is given as

$$U = \frac{1}{2}\int_A \int_{-h/2}^{h/2} \sum_{i=1}^{N} (\sigma_{ix}\varepsilon_{ix} + \sigma_{iy}\varepsilon_{iy} + \sigma_{ixy}\gamma_{ixy})\, dz\, dA \tag{2.8}$$

where σ_{ix}, σ_{iy}, σ_{ixy} are the corresponding stresses for the above strains.

The internal forces and moments exerted on the mid-plane are written as

$$\begin{aligned} [N_{ix}, N_{iy}, N_{ixy}] &= \int_{-h/2}^{h/2} [\sigma_{ix}, \sigma_{iy}, \sigma_{ixy}]\, dz \\ [M_{ix}, M_{iy}, M_{ixy}] &= \int_{-h/2}^{h/2} [\sigma_{ix}, \sigma_{iy}, \sigma_{ixy}] z\, dz \end{aligned} \tag{2.9}$$

Substituting the mid-plane forces and moments into Eq. (2.8), we get

$$U = \frac{1}{2}\int_A \sum_{i=1}^{N} (N_{ix}\varepsilon_{ix0} + M_{ix}\kappa_{ix} + N_{iy}\varepsilon_{iy0} + M_{iy}\kappa_{iy} + N_{ixy}\varepsilon_{ixy0} + M_{ix}\kappa_{ixy})\, dA \tag{2.10}$$

The kinetic energy T is given by

$$T = \frac{\rho}{2}\int_A \int_{-h/2}^{h/2} \sum_{i=1}^{N} \Big[\Big(\frac{\partial \overline{u}_i}{\partial t}\Big)^2 + \Big(\frac{\partial \overline{v}_i}{\partial t}\Big)^2 + \Big(\frac{\partial \overline{w}_i}{\partial t}\Big)^2\Big]\, dz\, dA \tag{2.11}$$

where ρ is density of the graphene sheet.

The work done by van der Waals forces is given by

$$V = \int_A F_i w_i\, dA = \int_A \Big(\sum_{j=1,\, j\neq i}^{N} [c_{ij}(w_i - w_j) + \overline{c}_{ij}(w_i - w_j)^3] \Big) w_i\, dA \tag{2.12}$$

According to Hamilton's principle, the equations of motion of the orthotropic nanoplate is given by

$$\int_0^t \delta(T - U + V)\, dt = 0 \tag{2.13}$$

where T, U, V are kinetic energy, strain energy and potential energy, respectively.

Substituting T, U and V and neglecting the longitudinal and in plane inertial forces, leads to the following equation of motion (Jomehzadeh and Saidi, 2011)

$$\frac{\partial N_{ix}}{\partial x} + \frac{\partial N_{ixy}}{\partial y} = 0 \qquad \frac{\partial N_{ixy}}{\partial x} + \frac{\partial N_{iy}}{\partial y} = 0 \tag{2.14}$$

and

$$\begin{aligned}\frac{\partial^2 M_{ix}}{\partial x^2}+2\frac{\partial^2 M_{ixy}}{\partial x\partial y}+\frac{\partial^2 M_{iy}}{\partial y^2}+\frac{\partial}{\partial x}\Big(N_{ix}\frac{\partial w_i}{\partial x}+N_{ixy}\frac{\partial w_i}{\partial y}\Big)+\frac{\partial}{\partial y}\Big(N_{ixy}\frac{\partial w_i}{\partial x}+N_{iy}\frac{\partial w_i}{\partial y}\Big)\\ =\sum_{j=1,\,j\neq i}^{N}[c_{ij}(w_i-w_j)+\overline{c}_{ij}(w_i-w_j)^3]+I_0\frac{\partial^2 w_i}{\partial t^2}-I_2\Big(\frac{\partial^4 w_i}{\partial x^2\partial t^2}+\frac{\partial^4 w_i}{\partial y^2\partial t^2}\Big)\end{aligned} \tag{2.15}$$

where I_0 and I_2 are the inertia parameters expressed as

$$(I_0, I_2)=\int_{-h/2}^{h/2}\rho(1,z^2)\,dz \tag{2.16}$$

Applying the nonlocal theory from Eq. (2.1), the nonlocal stress relationships are obtained as

$$(1-\mu^2\nabla^2)\begin{Bmatrix}\sigma_{ix}\\ \sigma_{iy}\\ \sigma_{ixy}\end{Bmatrix}=\begin{bmatrix}C_{11}&C_{12}&0\\ C_{12}&C_{22}&0\\ 0&0&C_{66}\end{bmatrix}\begin{Bmatrix}\varepsilon_{ix}\\ \varepsilon_{iy}\\ \gamma_{ixy}\end{Bmatrix} \tag{2.17}$$

where C_{ij} is elastic constants of the graphene layer, and $\mu=e_0a$.

Substituting the above stress relations to Eq. (2.9), the resultant forces and moments become

$$\begin{aligned}(1-\mu^2\nabla^2)\begin{Bmatrix}N_{ix}\\ N_{iy}\\ N_{ixy}\end{Bmatrix}&=\begin{bmatrix}A_{11}&A_{12}&0\\ A_{12}&A_{22}&0\\ 0&0&A_{66}\end{bmatrix}\begin{Bmatrix}\varepsilon_{ix0}\\ \varepsilon_{iy0}\\ \gamma_{ixy0}\end{Bmatrix}\\ (1-\mu^2\nabla^2)\begin{Bmatrix}M_{ix}\\ M_{iy}\\ M_{ixy}\end{Bmatrix}&=\begin{bmatrix}D_{11}&D_{12}&0\\ D_{12}&D_{22}&0\\ 0&0&D_{66}\end{bmatrix}\begin{Bmatrix}\kappa_{ix}\\ \kappa_{iy}\\ \kappa_{ixy}\end{Bmatrix}\end{aligned} \tag{2.18}$$

where A_{ij} and D_{ij} represent the stretching stiffness and bending stiffness respectively, and are given by

$$A_{ij}=\int_{-h/2}^{h/2}C_{ij}\,dz \qquad D_{ij}=\int_{-h/2}^{h/2}z^2C_{ij}\,dz \tag{2.19}$$

Airy's stress function Φ is introduced so that it satisfies equation of motion (2.14)

$$N_{ix}=\frac{\partial^2\Phi_i}{\partial y^2} \qquad N_{iy}=\frac{\partial^2\Phi_i}{\partial x^2} \qquad N_{ixy}=-\frac{\partial^2\Phi_i}{\partial x\partial y} \tag{2.20}$$

Multiplying Eq. (2.15) by $(1-\mu^2\nabla^2)$ and substituting the nonlocal resultant force and moment, Eqs. (2.18), and the stress function from Eq. (2.20), the nonlocal governing differential equation of motion is obtained as (Jomehzadeh and Saidi, 2011)

$$\begin{aligned}&D_{11}\frac{\partial^4 w_i}{\partial x^4}+2(D_{12}+2D_{66})\frac{\partial^4 w_i}{\partial x^2\partial y^2}+D_{22}\frac{\partial^4 w_i}{\partial y^4}+(1-\mu^2\nabla^2)\Big[I_0\frac{\partial^2 w_i}{\partial t^2}\\ &-I_2\Big(\frac{\partial^4 w_i}{\partial x^2\partial t^2}+\frac{\partial^4 w_i}{\partial y^2\partial t^2}\Big)\Big]-(1-\mu^2\nabla^2)\sum_{j=1,\,j\neq i}^{N}[c_{ij}(w_i-w_j)+\overline{c}_{ij}(w_i-w_j)^3]\\ &-(1-\mu^2\nabla^2)\Big(\frac{\partial^2 w_i}{\partial x^2}\frac{\partial^2\Phi_i}{\partial y^2}+\frac{\partial^2 w_i}{\partial y^2}\frac{\partial^2\Phi_i}{\partial x^2}-2\frac{\partial^2 w_i}{\partial x\partial y}\frac{\partial^2\Phi_i}{\partial x\partial y}\Big)=0\end{aligned} \tag{2.21}$$

The above equation is a function of transverse displacement and stress. To solve the above equation, the compatibility of mid-plane is employed, and is given as

$$\frac{\partial^2 \varepsilon_{ix}}{\partial y^2} + \frac{\partial^2 \varepsilon_{iy}}{\partial x^2} - \frac{\partial^2 \gamma_{ixy}}{\partial x \partial y} = \Big(\frac{\partial^2 w_i}{\partial x \partial y}\Big)^2 - \frac{\partial^2 w_i}{\partial x^2}\frac{\partial^2 w_i}{\partial y^2} \tag{2.22}$$

Substituting the stress functions from Eq. (2.20) to the above equation, the compatibility equation in terms of the stress function is given as

$$S_{11}\frac{\partial^4 \Phi_i}{\partial x^4} + 2(S_{12} + 2S_{66})\frac{\partial^4 \Phi_i}{\partial x^2 \partial y^2} + S_{22}\frac{\partial^4 \Phi_i}{\partial y^4} = \Big(\frac{\partial^2 w_i}{\partial x \partial y}\Big)^2 - \frac{\partial^2 w_i}{\partial x^2}\frac{\partial^2 w_i}{\partial y^2} \tag{2.23}$$

where S_{ij} represent components of the inverse of the stretching stiffness matrix $\mathbf{A}$.

3. Solution

A simply supported (SSSS) boundary condition for geometrical larger deformation of MLGS is considered. For the simply supported edges, the boundary conditions are written as:
— at $x = \pm a/2$

$$w_i(x,y) = 0 \qquad M_{ix} = 0 \qquad \frac{\partial^2 \Phi_i}{\partial x \partial y} = 0 \qquad \int\limits_{-b/2}^{b/2} \frac{\partial^2 \Phi_i}{\partial y^2}\, dy = 0 \tag{3.1}$$

— at $y = \pm b/2$

$$w_i(x,y) = 0 \qquad M_{iy} = 0 \qquad \frac{\partial^2 \Phi_i}{\partial x \partial y} = 0 \qquad \int\limits_{-a/2}^{a/2} \frac{\partial^2 \Phi_i}{\partial x^2}\, dx = 0 \tag{3.2}$$

To satisfy the above simply supported boundary conditions, the nonlinear vibration deflections for each layer of MLGS are given by

$$(w_{mn})_i = hW_i(t)\sin\frac{m\pi x}{a}\sin\frac{n\pi y}{b} \tag{3.3}$$

where $W_i(t)$ is the dimensionless amplitude of vibration.

Substituting Eq. (3.3) into Eq. (2.23) and solving for Φ_i, the stress function Φ_i is obtained as (Jomehzadeh *et al.*, 2012)

$$\Phi_i = \Big(\frac{h^2 a^2 n^2}{32 b^2 n^2 S_{11}}\cos\frac{2m\pi x}{a} + \frac{h^2 b^2 m^2}{32 a^2 n^2 S_{22}}\cos\frac{2n\pi y}{b}\Big)W_i(t)^2 \tag{3.4}$$

Substituting the transverse displacement from Eq. (3.3) and the stress function from Eq. (3.4) into the governing equation Eq. (2.21), and then using the Galerkin method, the modal equations are obtained as

$$\frac{\partial^2 W_i(t)}{\partial t^2} + \sum_{j=1}^{N}\alpha_{ij}W_j(t) + \beta_i W_i(t)^3 + \sum_{j=1,\, j\neq i}^{N}\mathcal{V}_{ij}[W_i(t) - W_j(t)]^3 = 0 \tag{3.5}$$

The coefficients α_{ii}, α_{ij}, β_i and $\mathcal{V}_{ij}$ are given as

$$\alpha_{ii} = \frac{\pi^4[a^4 D_{22} m^4 + 2a^2b^2m^2n^2(D_{121}+2D_{33}) + b^4 D_{11} n^4]}{[\pi^2\mu^2(a^2m^2+b^2n^2)+a^2b^2][a^2b^2I_0+\pi^2 I_2(a^2m^2+b^2n^2)]} + \frac{a^2b^2\sum_{j=1,\, j\neq i}^{N} c_{ij}}{a^2b^2I_0+\pi^2 I_2(a^2m^2+b^2n^2)}$$

$$\alpha_{ij} = -\frac{a^2b^2 c_{ij}}{a^2b^2I_0+\pi^2 I_2(a^2m^2+b^2n^2)} \qquad \mathcal{V}_{ij} = \frac{9a^2b^2\overline{c}_{ij}h^2}{16[a^2b^2I_0+\pi^2 I_2(a^2m^2+b^2n^2)]}$$

$$\beta_i = \frac{\pi^4 h^2(a^4 S_{11} m^4 + S_{22} b^4 n^4)}{16a^2 S_{11} S_{22} b^2[a^2b^2I_0+\pi^2 I_2(a^2m^2+b^2n^2)]}$$

The solution to the above coupled Duffing type equation can be written as

$$W_i(t) = a_i \mathrm{Cn}(\omega t, \overline{m}) \tag{3.6}$$

where Cn is the elliptical cosine function, $\overline{m}$ is the elliptic modulus and a_i is the maximum amplitude of i-th layer. Substituting the solution to equation (3.5), and performing simple mathematical operations, we get

$$\left[(2\overline{m}-1)\omega^2 + \alpha_{ii} + \sum_{j=1}^{N}\alpha_{ij}\frac{a_j}{a_i}\right]W_i(t) + \left[\beta_i - \frac{2\overline{m}\omega^2}{a_i^2} + \sum_{j=1}^{N}\mathcal{V}_{ij}\Big(1-\frac{a_j}{a_i}\Big)^3\right]W_i(t)^3 = 0 \tag{3.7}$$

To get a unique solution in all the time, the coefficients of all $W_i(t)$ and $W_i(t)^3$ must be zero. Equating all $W_i(t)$ and $W_i(t)^3$ to zero, we write

$$(2\overline{m}-1)\omega^2 + \alpha_{ii} + \sum_{j=1}^{N}\alpha_{ij}\frac{a_j}{a_i} = 0 \qquad \beta_i - \frac{2\overline{m}\omega^2}{a_i^2} + \sum_{j=1}^{N}\mathcal{V}_{ij}\Big(1-\frac{a_j}{a_i}\Big)^3 = 0 \tag{3.8}$$

Solving the above equations for ω and $\overline{m}$ results in

$$\omega_i = \sqrt{\left(\alpha_{ii} + \sum_{j=1,\, j\neq i}^{N}\alpha_{ij}\frac{a_j}{a_i}\right) + \left(\beta_i + \sum_{j=1,\, j\neq i}^{N}\mathcal{V}_{ij}\frac{(a_i-a_j)^3}{a_i^3}\right)a_i^2}$$

$$\overline{m}_i = \frac{\left(\beta_i + \sum_{j=1,\, j\neq i}^{N}\mathcal{V}_{ij}\frac{(a_i-a_j)^3}{a_i^3}\right)a_i^2}{2\left[\left(\alpha_{ii} + \sum_{j=1,\, j\neq i}^{N}\alpha_{ij}\frac{a_j}{a_i}\right) + \left(\beta_i + \sum_{j=1,\, j\neq i}^{N}\mathcal{V}_{ij}\frac{(a_i-a_j)^3}{a_i^3}\right)a_i^2\right]} \tag{3.9}$$

The nonlinear frequency is expressed as

$$\omega_{nli} = \frac{\pi/2}{K(\overline{m}_i)}\omega_i \tag{3.10}$$

where $K(\overline{m})$ is a complete elliptical integral of the first kind, and is given by

$$K(\overline{m}) = \int_0^{\pi/2}\frac{d\theta}{\sqrt{1-\overline{m}\sin^2\theta}} \tag{3.11}$$

The solution for SLGS is obtained by substituting $N=1$ and $c_{ij} = \overline{c}_{ij} = 0$ into Eq. (3.9)

$$\omega = \sqrt{\alpha_{11}+\beta_1 a^2} \qquad \overline{m} = \frac{\beta_1 a^2}{2(\alpha_{11}+\beta_1 a^2)} \tag{3.12}$$

The solution for DLGS is obtained by substituting $N = 2$ in Eq. (3.9) as

$$\omega_1 = \sqrt{\Big(\alpha_{11} + \alpha_{12}\frac{a_2}{a_1}\Big) + \Big[\beta_1 + \mathcal{V}_{12}\Big(1 - \frac{a_2}{a_1}\Big)^3\Big]a_1^2} \qquad \overline{m}_1 = \frac{\Big[\beta_1 + \mathcal{V}_{12}\Big(1 - \frac{a_2}{a_1}\Big)^3\Big]a_1^2}{2\omega_1^2}$$
$$\omega_2 = \sqrt{\Big(\alpha_{22} + \alpha_{21}\frac{a_1}{a_2}\Big) + \Big[\beta_2 + \mathcal{V}_{21}\Big(1 - \frac{a_1}{a_2}\Big)^3\Big]a_2^2} \qquad \overline{m}_2 = \frac{\Big[\beta_2 + \mathcal{V}_{21}\Big(1 - \frac{a_1}{a_2}\Big)^3\Big]a_2^2}{2\omega_2^2} \tag{3.13}$$

The frequency of vibration must be unique for a physical system. Equating $\omega_1 = \omega_2$, the relationship between a_1 and a_2 is found as

$$\Big(\alpha_{11} + \alpha_{12}\frac{a_2}{a_1}\Big) + \Big[\beta_1 + \mathcal{V}_{12}\Big(1 - \frac{a_2}{a_1}\Big)^3\Big]a_1^2 = \Big(\alpha_{22} + \alpha_{21}\frac{a_1}{a_2}\Big) + \Big[\beta_2 + \mathcal{V}_{21}\Big(1 - \frac{a_1}{a_2}\Big)^3\Big]a_2^2 \tag{3.14}$$

The first solution for TLGS is obtained by substituting $N = 3$ in Eq. (3.9) as

$$\omega_1 = \sqrt{\Big(\alpha_{11} + \alpha_{12}\frac{a_2}{a_1} + \alpha_{13}\frac{a_3}{a_1}\Big) + \Big[\beta_1 + \mathcal{V}_{12}\Big(1 - \frac{a_2}{a_1}\Big)^3 + \mathcal{V}_{13}\Big(1 - \frac{a_3}{a_1}\Big)^3\Big]a_1^2}$$
$$\overline{m}_1 = \frac{\Big[\beta_1 + \mathcal{V}_{12}\Big(1 - \frac{a_2}{a_1}\Big)^3 + \mathcal{V}_{13}\Big(1 - \frac{a_3}{a_1}\Big)^3\Big]a_1^2}{2\Big\{\Big(\alpha_{11} + \alpha_{12}\frac{a_2}{a_1} + \alpha_{13}\frac{a_3}{a_1}\Big) + \Big[\beta_1 + \mathcal{V}_{12}\Big(1 - \frac{a_2}{a_1}\Big)^3 + \mathcal{V}_{13}\Big(1 - \frac{a_3}{a_1}\Big)^3\Big]a_1^2\Big\}} \tag{3.15}$$

Similarly, ω_2, $\overline{m}_2$ and ω_3, $\overline{m}_3$ is found. The relationship between a_1, a_2 and a_3 is found by equating $\omega_1 = \omega_2 = \omega_3$.

4. Results and discussions

To verify the validation of the present formulations, comparision between the frequencies for present method and the model by He *et al.* (2005) is presented in Table 1 for the double and eight layer square graphene sheets. From Table 1, it is seen that the proposed formulation has a good agreement with the literature. Furtherly, the nonlinear frequency for a simply supported armchair SLGS is compared with the harmonic balance method from the reference by Jomehzadeh *et al.* (2012), and is shown in Fig. 3. From Fig. 3, it is seen that the present formulation has a good agreement with the harmonic balance method.

For SLGS and MLGS, the value of e_0a was found to vary based on the initial stress, rotating inertia, mode shape and the aspect ratio of rectangular plates. However, Eringen proposed the small scale parameter as 0.39 (Eringen, 1983). For SLGS, Shen *et al.* (2010) conducting molecular dynamics simulations, and found that the small scale parameter $e_0a = 0.67\,\text{nm}$ corresponds to sheet configuration. In general, a conservative estimate of the nonlocal parameter for SWCNTs is $e_0a < 2.0\,\text{nm}$ (Huang *et al.*, 2012). Hence, the small scale effects on the vibration behaviour of graphene sheets were carried out analytically by assuming the range of values $e_0a = 0\,\text{nm}$ to $1.5\,\text{nm}$.

The numerical results are given in this paper for simply supported graphene sheets with material properties and dimensions according to Jomehzadeh *et al.* (2012).

From Eq. (3.12), it is evident that an increase in the amplitude increases ω. Figure 3b shows the same. The coefficient α_{11} is inversely proportional to the nonlocal parameter μ. Hence, an increase in the nonlocal parameter decreases α_{11}, thereby diminishes the nonlinear frequency. Figure 3b shows that an increase in the nonlocal parameter decreases the nonlinear frequency.

Table 1. Natural frequencies [THz] for double and eight-layered square GSs

A	B		$m=1$			$m=2$			$m=3$		
			$n=1$	$n=2$	$n=3$	$n=1$	$n=2$	$n=3$	$n=1$	$n=2$	$n=3$
2	ω_1	Ref.	0.069	0.173	0.346	0.173	0.276	0.449	0.346	0.449	0.622
		Present	0.067	0.166	0.332	0.166	0.266	0.432	0.332	0.432	0.597
	ω_2	Ref.	2.683	2.688	2.705	2.688	2.697	2.720	2.705	2.720	2.754
		Present	2.681	2.681	2.690	2.681	2.685	2.701	2.690	2.701	2.726
8	ω_1	Ref.	0.069	0.173	0.346	0.173	0.276	0.449	0.346	0.449	0.622
		Present	0.067	0.166	0.332	0.166	0.266	0.432	0.332	0.432	0.597
	ω_2	Ref.	0.713	0.730	0.789	0.730	0.761	0.840	0.789	0.840	0.944
		Present	0.712	0.727	0.780	0.727	0.755	0.827	0.780	0.827	0.923
	ω_3	Ref.	1.407	1.416	1.447	1.416	1.433	1.476	1.447	1.476	1.537
		Present	1.406	1.412	1.438	1.412	1.425	1.462	1.438	1.462	1.516
	ω_4	Ref.	2.063	2.069	2.090	2.069	2.080	2.110	2.090	2.110	2.153
		Present	2.060	2.063	2.078	2.063	2.071	2.094	2.078	2.094	2.129
	ω_5	Ref.	2.647	2.652	2.669	2.652	2.661	2.684	2.669	2.684	2.718
		Present	2.645	2.645	2.655	2.645	2.650	2.665	2.655	2.665	2.691
	ω_6	Ref.	3.133	3.137	3.151	3.137	3.144	3.164	3.151	3.164	3.193
		Present	3.130	3.129	3.135	3.129	3.131	3.142	3.135	3.142	3.162
	ω_7	Ref.	3.495	3.498	3.511	3.498	3.505	3.523	3.511	3.523	3.549
		Present	3.491	3.490	3.493	3.490	3.491	3.499	3.493	3.499	3.515
	ω_8	Ref.	3.717	3.720	3.732	3.720	3.726	3.743	3.732	3.743	3.768
		Present	3.713	3.711	3.713	3.711	3.712	3.71	3.713	3.718	3.733

A – number of layers; B – natural frequencies; Ref. – He *et al.* (2005)

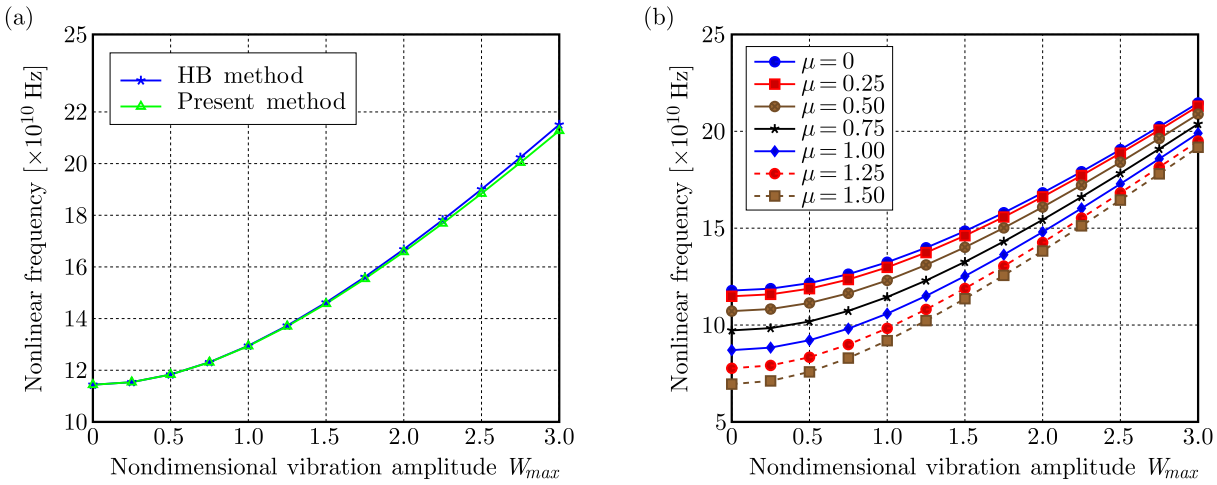

Fig. 3. (a) Comparison of the harmonic balance method and the present method. (b) Variation of the monlinear frequency of SLGS for different nonlocal parameter

Figure 4a shows variation of the frequency ratio for different nonlocal parameters. The linear nonlocal frequency, which is equal to $\sqrt{\alpha_{11}}$, decreases with an increase in the nonlocal parameter. Hence, the frequency ratio ω_{nl}/ω_l increases with the nonlocal parameter. This is because a decrease in the nonlinear frequency is less than the decrease in the linear frequency, and hence the frequency ratio increases with the nonlocal parameter. From the above discussion, it is evident that the nonlinear frequency decreases with an increase in the nonlocal parameter, but the frequency ratio increases with an increase in the nonlocal parameter.

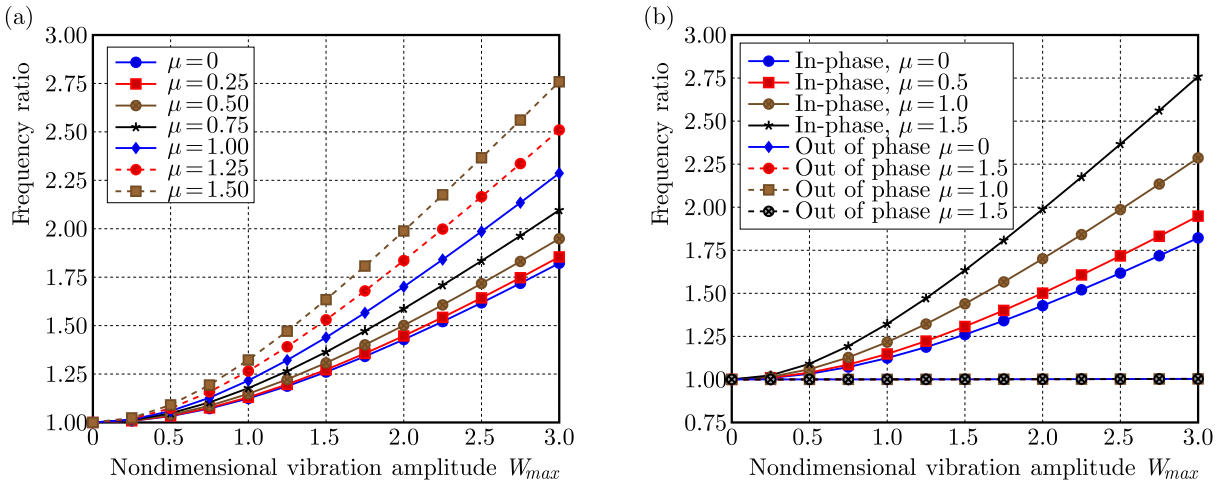

Fig. 4. (a) Variation of the frequency ratio of SLGS with the amplitude. (b) Variation of the frequency ratio of DLGS for various nonlocal parameters μ for the linear van der Waals force

The solution to the DLGS amplitude relationship, from Eq. (3.14), is $a_2 = a_1$ and $a_2 = -a_1$. The first solution $a_2 = a_1$ gives an in-phase frequency of vibration, and $a_2 = -a_1$ gives out-of-phase frequency of the vibration. The elliptic modulus and nonlinear vibration frequency for the in-phase vibration is given by

$$\omega = \sqrt{\alpha_{11} + \alpha_{12} + \beta_1 a^2} \qquad \overline{m} = \frac{\beta_1 a^2}{2(\alpha_{11} + \alpha_{12} + \beta_1 a^2)} \tag{4.1}$$

In the above equation, $\alpha_{11} + \alpha_{12} = \alpha_{11}$ (with $c_{ij} = 0$), which is a solution to SLGS. Hence, it is proved that the nonlinear in-phase frequency of DLGS is the same as that of SLGS, and is independent of the linear van der Waals coefficient. Hence, Fig. 4b shows the variation of the in-phase frequency ratio, which is similar to that of SLGS.

Substituting the out-of-phase amplitude solution and $\mathcal{V}_{12} = 0$, the nonlinear out-of-phase frequency and elliptic modulus for the linear van der Waals force are given by

$$\omega_1 = \sqrt{(\alpha_{11} - \alpha_{12}) + \beta_1 a_1^2} \qquad \overline{m}_1 = \frac{\beta_1 a_1^2}{2(\alpha_{11} - \alpha_{12}) + \beta_1 a_1^2]} \tag{4.2}$$

In the above equation, $\alpha_{11} - \alpha_{12}$ depends on the linear van der Waals coefficient. Hence, both linear and nonlinear frequencies vary similarly with the van der Waals coefficient. The change in the frequency ratio is insignificant. Figure 4b shows the same.

Figure 5a shows the effect of the nonlocal parameter for the in-phase frequency including the nonlinear van der Waals force coefficient. The nonlinear vibration solution including the nonlinear van der Waals force coefficent for the in-phase frequency is given by

$$\omega_1 = \sqrt{(\alpha_{11} + \alpha_{12}) + (\beta_1 + 8\mathcal{V}_{12})a_1^2} \qquad \overline{m}_1 = \frac{(\beta_1 + 8\mathcal{V}_{12})a_1^2}{2[(\alpha_{11} + \alpha_{12}) + (\beta_1 + 8\mathcal{V}_{12})a_1^2]} \tag{4.3}$$

From the above relation, it is evident that the in-phase frequency is independent of the linear van der Waals coefficient and vary much with it. Hence, the frequency ratio is much increased with an increase in W_{max}. Since μ depends on α_{11} only, the variation in the frequency ratio is similar to that of SLGS.

Substituting the out-of-phase amplitude solution, the nonlinear frequency of vibration and elliptic modulus for the nonlinear van der Waals force are given by

$$\omega_1 = \sqrt{(\alpha_{11} - \alpha_{12}) + (\beta_1 + 8\mathcal{V}_{12})a_1^2} \qquad \overline{m}_1 = \frac{(\beta_1 + 8\mathcal{V}_{12})a_1^2}{2[(\alpha_{11} - \alpha_{12}) + (\beta_1 + 8\mathcal{V}_{12})a_1^2]} \tag{4.4}$$

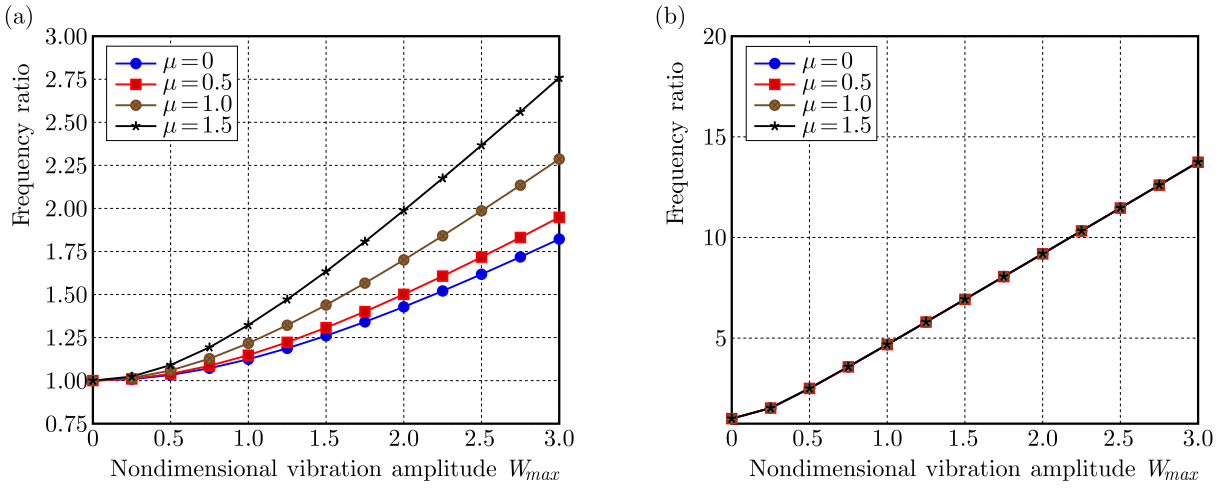

Fig. 5. Variation of the frequency ratio of DLGS including the nonlinear van der Waals force for (a) in-phase frequency, (b) out-of-phase frequency

From the above solution, it is clear that the out-of-phase frequency ratio variation is similar to the linear van der Waals force. Figure 5b shows the effect of the nonlocal parameter on the frequency ratio including the nonlinear van der Waals force for the out-of-phase frequency. The figure shows that the nonlocal parameter does not have any significant effect on the frequency ratio, unlike the in-phase frequency.

To study the linear and nonlinear effects of van der Waals forces, backbone curves are drawn for a nonlocal parameter $\mu = 0.5$. Figure 6a shows the variation of nonlinear frequency for the linear and nonlinear, in-phase and out-of-phase frequency. From Fig. 6a, the in-phase frequency is the same for the linear and nonlinear frequency. But the nonlinear van der Waals forces have a significant effect on the vibration out-of-phase frequency.

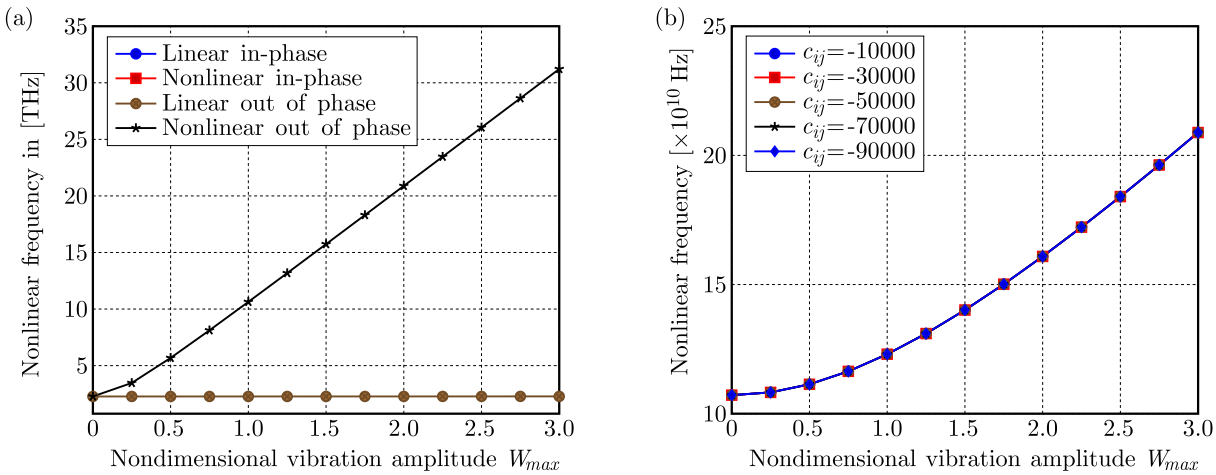

Fig. 6. (a) Nonlinear frequency variation for the linear and nonlinear van der Waals forces for in-phase and out-of-phase vibrations. (b) Effect of $\overline{c}_{ij}$ on the in-phase frequency

Figure 6b shows the effect of the nonlinear coefficient $\overline{c}_{ij}$ for the in-phase and out-of-phase frequency. For the in-phase frequency, the solution $a_2 = a_1$ is substituted into the nonlinear vibration solution. The solution is independent of $\mathcal{V}$, which is a function of $\overline{c}_{ij}$. Hence, the in-phase nonlinear coefficient does not have any effect on the nonlinear frequency curve. For the out-of-phase frequency, the solution $a_2 = -a_1$ is substituted into the nonlinear vibration solution. The out-of-phase frequency depends on the nonlinear van der Waals coefficient.

Figure 7a shows the variation of nonlinear frequency with the nonlinear van der Waals coefficient for the out-of-phase frequency. From Fig. 7a, it is evident that am increase in the nonlinear van der Waals coefficient increases the nonlinear frequency.

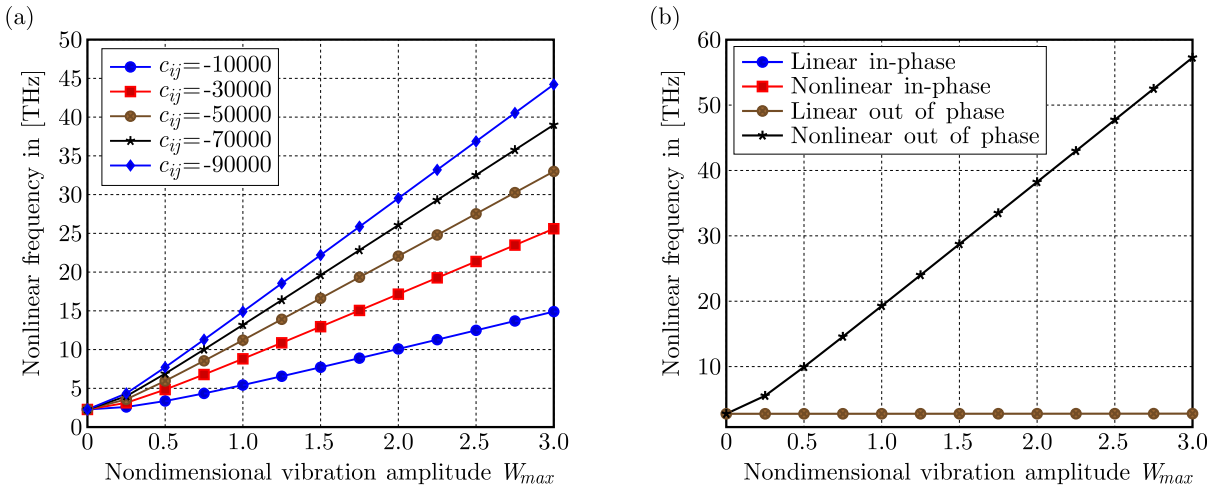

Fig. 7. (a) Effect of $\overline{c}_{ij}$ on the out-of-phase frequency. (b) Nonlinear frequency of linear and nonlinear van der Waals forces of TLGS

The solution of the TLGS amplitude relationship is found by equating the nonlinear frequencies $\omega_1 = \omega_2 = \omega_3$ as $a_1 = a_3 = a_2$ for in-phase and $a_1 = a_3 = -2a_2$ for out-of-phase vibrations. Unlike DLGS, in TLGS and all other higher MLGS, the out-of-phase frequency is not obtained from $a_2 = -a_1$ since the stiffness contribution for each layer is different.

Like DLGS, TLGS (and all MLGS) the in-phase frequency is obtained from $a_i = a_1$. This gives the vibration frequency, similar to SLGS, as discussed above in DLGS. Hence, it is proved that the in-phase frequency of vibration does not change for TLGS, and MLGS, irrespective of the number of layers. Figure 7b shows the nonlinear and linear in-phase and out-of-phase frequency ratios. The out-of-phase frequency is much dependent on nonlinear van der Waals forces, as discussed in DLGS. But variation of the out-of-phase frequency is greater in TLGS than DLGS. Hence, an increase in the number of layers, the nonlinear van der Waals force increases the nonlinear frequency to a great extent.

5. Conclusion

Based on Eringen nonlocal elasticity theory and von Karman geometric non-linearity, free vibration analysis of Multilayer Graphene Sheets has been formulated. The nonlinear governing equations are obtained using Hamilton's principle. The nonlinear coupled equations of motion for simply supported boundary conditions are uncoupled using elliptical functions. The exact relationship between the nonlinear frequency, elliptic modulus and amplitude of vibration of SLGS, DLGS, TLGS and MLGS is derived and explained for its relationship with the in-phase, out-of-phase frequency for linear and nonlinear van der Waals forces.

The results show that the small scale parameter does not have any significant effect on the out-of-phase frequency ratio, whereas it influences the in-phase frequency ratio. The nonlinear van der Waals force does not have any significant effect on the in-phase frequency, whereas it changes the out-of-phase frequency much. The nonlinear van der Waals force coefficient between two layers has a significant effect on both the in-phase and out-of-phase nonlinear frequencies.

An analytical presentation provides a better understanding of the system features and makes it easier to draw broad generalizations. Another potential application of analytical solution offers reliable reference data for a numerical evaluation method. The exact analytical results reported here are thought to be useful.

References

1. Ansari R., Rajabiehfard R., Arash B., 2010, Nonlocal finite element model for vibrations of embedded multi-layered graphene sheets, *Computational Materials Science*, **49**, 4, 831-838
2. Arash B., Wang Q., 2011, Vibration of single- and double-layered graphene sheets, *Journal of Nanotechnology in Engineering and Medicine*, **2**, 1
3. Asghari M., 2012, Geometrically nonlinear micro-plate formulation based on the modified couple stress theory, *International Journal of Engineering Science*, **51**, 292-309
4. Behfar K., Naghdabadi R., 2005, Nanoscale vibrational analysis of a multi-layered graphene sheet embedded in an elastic medium, *Composites Science and Technology*, **65**, 7-8, 1159-1164
5. Eringen A.C., 1983, On differential equations of nonlocal elasticity and solutions of screw dislocation and surface waves, *Journal of Applied Physics*, **54**, 9, 4703-4710
6. Farajpour A., Ghayesh M.H., Farokhi H., 2018, A review on the mechanics of nanostructures, *International Journal of Engineering Science*, **133**, 231-263
7. Ghannadpour S.A.M., Moradi F., 2019, Nonlocal nonlinear analysis of nano-graphene sheets under compression using semi-Galerkin technique, *Advances in Nano Research*, **7**, 5, 311-324
8. Ghayesh M.H., Farokhi H., 2015, Nonlinear dynamics of microplates, *International Journal of Engineering Science*, **86**, 60-73
9. He X.Q., Kitipornchai S., Liew K.M.. 2005, Resonance analysis of multi-layered graphene sheets used as nanoscale resonators, *Nanotechnology*, **16**, 10, 2086-2091
10. Huang L.Y., Han Q., Liang Y.J., 2012, Calibration of nonlocal scale effect parameter for bending single-layered graphene sheet under molecular dynamics, *Nano*, **7**, 5, 1250033
11. Jomehzadeh E., Saidi A.,R., 2011, A study on large amplitude vibration of multilayered graphene sheets, *Computational Materials Science*, **50**, 3, 1043-1051
12. Jomehzadeh E., Saidi A.R., Pugno N.M., 2012, Large amplitude vibration of a bilayer graphene embedded in a nonlinear polymer matrix, *Physica E: Low-Dimensional Systems and Nanostructures*, **44**, 10, 1973-1982
13. Kong S., Zhou S., Nie Z., Wang K., 2009, Static and dynamic analysis of micro beams based on strain gradient elasticity theory, *International Journal of Engineering Science*, **47**, 4, 487-498
14. Lam D.C.C., Yang F., Chong A.C.M., Wang J., Tong P., 2003, Experiments and theory in strain gradient elasticity, *Journal of the Mechanics and Physics of Solids*, **51**, 8, 1477-1508
15. Mianroodi J.R., Niaki S.A., Naghdabadi R., Asghari M., 2011, Nonlinear membrane model for large amplitude vibration of single layer graphene sheets, *Nanotechnology*, **22**, 30, 305703
16. Murmu T., Pradhan S.C., 2009, Vibration analysis of nano-single-layered graphene sheets embedded in elastic medium based on nonlocal elasticity theory, *Journal of Applied Physics*, **105**, 6
17. Nematollahi M.S., Mohammadi R., 2019, Geometrically nonlinear vibration analysis of sandwich nanoplates based on higher-order nonlocal strain gradient theory, *International Journal of Mechanical Sciences*, **156**, December 2018, 31-45
18. Pradhan S.C., Phadikar J.K., 2009, Small scale effect on vibration of embedded multilayered graphene sheets based on nonlocal continuum models, *Physics Letters, Section A: General, Atomic and Solid State Physics*, **373**, 11, 1062-1069

19. Shen L.E., Shen H.-S., Zhang C.-L., 2010, Nonlocal plate model for nonlinear vibration of single layer graphene sheets in thermal environments, *Computational Materials Science*, **48**, 3, 680-685

20. Wang B., Zhao J., Zhou S., 2010, A micro scale Timoshenko beam model based on strain gradient elasticity theory, *European Journal of Mechanics, A/Solids*, **29**, 4, 591-599

Manuscript received June 17, 2021; accepted for print September 8, 2021